NACA

RESEARCH MEMORANDUM

A STUDY OF THE CORRELATION BETWEEN FLIGHT AND WIND-TUNNEL BUFFETING LOADS

By Wilber B. Huston, A. Gerald Rainey, and Thomas F. Baker

Langley Aeronautical Laboratory
Langley Field, Va.

NATIONAL ADVISORY COMMITTEE
FOR AERONAUTICS
WASHINGTON
July 19, 1955
Declassified February 8, 1957

NATIONAL ADVISORY COMMITTEE FOR AERONAUTICS

RESEARCH MEMORANDUM

A STUDY OF THE CORRELATION BETWEEN FLIGHT AND WIND-TUNNEL BUFFETING LOADS

By Wilber B. Huston, A. Gerald Rainey, and Thomas F. Baker

SUMMARY

Comparison of the buffet loads measured on wind-tunnel models with loads measured in flight indicates that, during the course of the regular wind-tunnel testing program on a model, a simple strain-gage measurement can be made which can be used to predict the wing buffet loads on the airplane. The comparison is made for airplanes with swept and with unswept wings. The relation between buffet loads on a model and buffet loads on an airplane in flight is discussed from the standpoint of the input-output relationships of generalized harmonic analysis. The analysis of buffet load measurements on a statistical basis is outlined.

INTRODUCTION

In several of the wind tunnels, experiments have been under way to see whether some simple measurement could be made, preferably in the course of the regular wind-tunnel testing program, which would predict the buffeting loads encountered on the airplane. This paper is in the nature of a progress report on this investigation.

In a study of this sort it has been necessary to find a measure of the loads which despite the fluctuating character of buffeting would permit comparison of model and airplane results. The instrumentation has been based on electrical strain-gage bridges mounted at the wing root of both model and airplane. Statistical procedures have been used in the data reduction and some of the quantities used are illustrated in figure 1.

SYMBOLS

$A^2(\omega)$	admittance of elastic system
b	wing span

c	chord
C_L	lift coefficient
C_{L_α}	effective slope of lift curve for vibrating wing under conditions of separated flow
C_M	bending-moment coefficient
C_N	normal-force coefficient
f	frequency
q	dynamic pressure
t	time
T	time interval
c_n	section normal-force coefficient
$I^2(\omega)$	power spectral density function of buffet force
p	static atmospheric pressure
V	airspeed
y	spanwise coordinate
y_g	location of strain-gage station
F_s	a structural factor
S	area
S_1	effective area in bending
S_2	effective area in bending
M_w	mass of wing
M_1	effective mass of wing in bending
$w_1(y)$	normalized shape of first bending mode
M_{m1}	effective moment of wing mass outboard of strain-gage station

σ standard deviation, or root-mean-square value

γ ratio of damping to critical damping

ω circular frequency

Subscripts:

L shear

M moment

ANALYSIS OF FLUCTUATING DATA

The wavy line in figure 1 is a portion of a strain-gage record taken during buffeting. Maximum peak-to-peak values have been used in the past as a measure of magnitude, but this measure suffers from a number of disadvantages. If the fluctuations y_B are taken as variations about the mean line (dashed), a number of studies under constant conditions of lift and Mach number both in wind tunnels and in flight show that the fluctuations are normally distributed. In other words, buffeting is a particular type of a random process, a Gaussian process. For such a process a natural measure and one which is of a much more stable nature than a peak-to-peak value is the root-mean-square value or the standard deviation σ. In the tunnels, this measure is easily obtained from a strain-gage output with standard electrical techniques. In flight, buffeting is frequently encountered during maneuvers, and the buffeting intensity may change with flight condition. For the analysis of flight records, where as here the maneuver component is changing, it has been found feasible to separate the two components by using numerical methods, break the buffet component into a series of short intervals of say 1/2 second, determine the root-mean-square value over each as defined by the formula, and use it as a measure of intensity. Flight-load data obtained in this way have been used for comparison with the wind-tunnel data.

SCALING OF BUFFET LOADS

For comparison of flight and model loads, some sort of scale factor is required. For dynamic analyses, the complexity of this scale factor would depend upon the complexity of the dynamic systems involved. Although airplanes exhibit complex vibration patterns, there are indications that, in some instances at least, simplification is permissible for the analysis of buffeting. Shown in figure 2 are frequency analyses of the wing-root bending moments obtained on three different airplanes: the Douglas X-3 with unswept wing, the Douglas D-558-II with swept wing, and the Convair XF-92A with delta wing. The ordinate is the power spectral density of the wing bending moment as obtained by Tukey's numerical procedures (see ref. 1) or the equivalent electrical techniques. Each spectrum is characterized by a single large peak and is similar to the response of a lightly damped single-degree-of-freedom system. In each case this peak is that associated with first symmetrical wing bending. Other modes are excited but to a very much lesser extent and it appears that a dynamic analysis based on a single degree of freedom should at least take care of first-order effects.

A simple basis for scaling buffet loads, and one which has been frequently used for the analysis of buffet data, may be termed the static analogy. Just as static forces such as lift or bending moment are defined by dimensionless coefficients C_L and C_M in the equations

$$L = C_L q S \tag{1}$$

$$M = C_M q \frac{b}{2} S \tag{2}$$

the root-mean-square shear σ_L or root-mean-square bending moment σ_M could be expressed by similar buffeting coefficients:

$$\sigma_L = C_{L_B} q S \tag{3}$$

$$\sigma_M = C_{M_B} q \frac{b}{2} S \tag{4}$$

The dynamic analysis of buffeting has been considered in some detail in references 2 to 4. The method, that of generalized harmonic analysis, is illustrated in some detail in reference 4, which has provided the basis for the present study. The input force, the admittance of the elastic system, and the aerodynamic damping all vary with frequency. Lift fluctuations associated with the separated flow over the wing are expressed in terms of their frequency content by means of a spectrum which is a function not only of frequency but of reduced frequency $\omega c/V$,

$$L^2(\omega) = q^2 c^2 \frac{c}{V} c_n\left(\frac{\omega c}{V}\right) \tag{5}$$

The admittance is that for a single-degree-of-freedom system,

$$A^2(\omega) = \frac{1}{\left(1 - \frac{\omega^2}{\omega_1^2}\right)^2 + \left(2\gamma \frac{\omega}{\omega_1}\right)^2} \tag{6}$$

The damping expressed in terms of critical damping is aerodynamic of the sort which is proportional to the angle-of-attack changes induced by the velocity of the bending vibrations and is specified by an effective slope of the lift curve c_{l_α} which is also a function of reduced frequency:

$$\gamma(\omega) = \frac{qc}{2m\omega_1 V} c_{l_\alpha}\left(\frac{\omega c}{V}\right) \tag{7}$$

These relationships may be used to compute the root-mean-square bending moment at the wing root

$$\sigma_M = \left[\omega_1 \frac{b}{2}\sqrt{\bar{c}SM_W}\right]\sqrt{q}\, F_S \left[\frac{C_N\left(\frac{\omega_1 \bar{c}}{V}\right)}{C_{L_\alpha}\left(\frac{\omega_1 \bar{c}}{V}\right)}\right]^{1/2} \tag{8}$$

In this expression (eq. (8)), the many parameters which enter have been grouped in several related terms. The first term in brackets includes the principal physical characteristics of the wing (natural frequency, span, chord, and mass). The operating conditions are represented by the square root of q. The quantity F_S is a dimensionless structural factor which reduces the actual values of wing area, mass, and moment arm to their effective values in the vibrating system. For a wing with spanwise chord distribution $c(y)$, the area S and two effective areas S_1 and S_2 are given by the expressions

$$S = \int_{-b/2}^{b/2} c(y)\,dy \tag{9}$$

$$S_1 = \int_{-b/2}^{b/2} c(y) w_1(y)\,dy \tag{10}$$

$$S_2 = \int_{-b/2}^{b/2} c(y) w_1^2(y)\,dy \tag{11}$$

where $w_1(y)$ is the shape of the fundamental wing-bending mode (taken as unity at the wing tips, $y = \pm b/2$). For a spanwise mass distribution $m(y)$, the wing mass M_w and an effective mass M_1 are defined by the integrals

$$M_w = \int_{-b/2}^{b/2} m(y)\,dy \tag{12}$$

$$M_1 = \int_{-b/2}^{b/2} m(y) w_1^2(y)\,dy \tag{13}$$

The effective moment of the mass outboard of the point y_g at which the strain-gage station is located is

$$M_{m_1} = \int_{y_g}^{b/2} (y - y_g) m(y) w_1(y)\,dy \tag{14}$$

and the structural factor F_S is given by the equation

$$F_S = \frac{M_{m_1}}{M_1 \frac{b}{2}} \sqrt{\frac{\pi}{8} \frac{S_1^2}{S_2 S} \frac{M_1}{M_w}} \tag{15}$$

The second term in brackets (eq. (8)) represents the magnitudes of the input spectrum and the damping at the particular value of reduced frequency corresponding to the fundamental bending frequency, the average chord, and the flight speed.

One simple basis for dynamic scaling is evident in equation (8). For both an airplane and its model, the factor F_S, depending primarily on plan form and mode shape, would be the same. If the reduced frequency of the model in the tunnel can be arranged to be the same as the flight value, the second term in brackets would also be the same. Thus in the ratio of the root-mean-square bending moment in flight to that of the model, the primary factor is the group of parameters included in the first bracket.

On the other hand, a more elaborate study could evaluate the reduced frequency function (second term in brackets) and it could be used as the basis for scaling. This parameter has been used in the flutter-tunnel study described subsequently.

One important distinction between the static and dynamic bases for scaling lies in the forms q and $\sqrt{q}$. An example of the use of statistical procedures for the analysis of flight buffeting loads which appears to discriminate neatly between the static and the dynamic case is provided by a recently completed analysis of some buffeting data on the North American F-86A, some of which are shown in figure 3.

CORRELATION OF BUFFET LOAD WITH FLIGHT CONDITION

Shown on the left-hand side of figure 3 are the values of C_N and Mach number during a typical gradual turn into buffeting. The circles represent conditions at successive one-second intervals. Also reproduced are half-second samples of an oscillograph record of a wing-root strain-gage bridge sensitive in this case primarily to shear. The leaders run to the average flight condition during the sample; the numbers 10 to 340 are the values of root-mean-square shear. There is a strong correlation between values of σ and C_N for this maneuver, as indicated by the plot on the right. This maneuver was performed at 35,000 feet. Similar data exist for a number of runs at this altitude at $M = 0.8$ and also at 45,000 feet. For wing-root bending moments, there are data at 20,000, 35,000, and 45,000 feet, some of which are shown in figure 4, where a comparison is made between the buffet loads at three different altitudes at $M = 0.8$. The root-mean-square bending moment is plotted against the static pressure on a log-log scale. The values and trends shown here, which are for a C_N of 0.65, are typical of those obtained with both shear and bending moment at other values of C_N. Straight lines with slopes proportional to p and $\sqrt{p}$ have been placed on the plot. Since Mach number is constant, these lines are also proportional to q and $\sqrt{q}$. The agreement shown with the $\sqrt{q}$ relationship confirms for a swept wing at transonic speeds the indications from an unswept wing reported in reference 4 and lends strong support to the validity of the dynamic approach to buffet scaling.

COMPARISON OF WIND-TUNNEL AND FLIGHT-TEST RESULTS

In figure 5 some buffet loads are given for a 1/16-scale model of the Douglas D-558-II measured in the Langley 7- by 10-foot tunnel. Shown are results for four different Mach numbers. The root-mean-square bending moment measured near the wing root at the 50-percent chord line has been measured with a strain-gage bridge and is plotted against lift coefficient. Circles represent runs made at the start of a general program on the model; squares represent a check run made at the middle of the general program; both show a good order of consistency. Straight lines have been faired through the data to represent what appear to be three typical characteristics. A low-level portion at low lift showing no change with lift occurs first; then there is a sharp increase with lift; and at the higher Mach numbers there is a further change in slope at still higher values of lift.

The low-level portion is believed to be associated with the residual tunnel turbulence. These tests were made following the installation of screens in the tunnel, a change which considerably improved the dynamic response of models although no change in static aerodynamic characteristics was noted. The increase in level is similar to that noted in flight on the F-86A. The change in slope was not noted on the F-86A tests but it occurs at values of lift which are higher than those reached in that study.

An important difference between the loads measured on the model in buffeting and those on the airplane is apparently associated with the model support system. The model was sting supported, the actual connection between sting and model being a six-component strain-gage balance. A frequency analysis of the model wing-root bending moment in buffeting is shown in figure 6. For the model as for the airplane, the bending moments in buffeting are largely associated with response in the first symmetrical wing bending mode, in this case centered on 196 cps, but another mode, which is a rocking motion of the model as a whole about the balance, is also present at about 80 cps. This physical restraint of roll by the balance represents a constraint and a vibrational mode which have no real counterparts in the buffet response of the airplane. The meter used to record the wing-root strain-gage output recorded the mean square of all components above about 5 cps. Frequency analyses (of which fig. 6 is typical) have been made of a few oscillograph records obtained during the tests at $M = 0.9$. These analyses indicate that roughly one-half of the mean-square bending moment is associated with the symmetrical bending mode. That is, on a square-root basis, the data of figure 5 at $M = 0.9$ may be considered as roughly 30 percent high for purposes of comparison with flight loads. It also appears that a simple correction could be made or a high-pass filter could be used to separate the symmetrical bending mode. Sufficient data are not now available, however, to adjust these data at all Mach numbers so that, for an extension to flight-test conditions, the faired lines were used to represent the wind-tunnel data, the low-level portion being ignored.

Shown in figure 7 is a comparison of the model loads of figure 5 scaled to the D-558-II airplane and compared with the root-mean-square bending moments measured in two gradual turns into buffeting at the average Mach numbers shown. The reduced frequencies of both model and airplane are nearly the same; the lines represent the 1/16-scale-model loads scaled to the flight conditions on the basis of the dynamic analysis incorporated in equation (8). The agreement between the scaled and flight data is considered to be encouraging.

In connection with figures 5 and 6, it was stated that the wind-tunnel data at $M = 0.9$ were of the order of 30 percent high because of the presence of model response in modes (especially the rocking mode at 80 cps) which have no counterpart in flight. The shaded area on the right-hand side of figure 7 is used to indicate where the model tests would fall if a simple correction were made for this effect. This comparison with flight loads is considered to be promising, especially when coupled with the results of a study under way in the Langley flutter tunnel shown in figures 8 and 9.

In figure 8 the ordinate is the value of root-mean-square bending moment in buffeting expressed in terms of the reduced-frequency buffeting parameter discussed in connection with the dynamic analysis

$$\left[\frac{C_N\left(\frac{\omega_1\bar{c}}{V}\right)}{C_{L_\alpha}\left(\frac{\omega_1\bar{c}}{V}\right)}\right]^{1/2}$$

The abscissa is the reduced frequency $\omega_1\bar{c}/V$ where ω_1 is the frequency of fundamental bending and $\bar{c}$, the average chord. These tests were run on a family of related unswept wings of the same geometry and airfoil section which differed only in stiffness and natural frequency and thus in the product $\omega_1\bar{c}$ shown. Each point represents a value of reduced frequency corresponding to a different speed. These data are for an angle of attack of 12°; data have been obtained for a number of different angles of attack. The variation with reduced frequency is typical. It is well represented by a mean line at higher values of $\omega_1\bar{c}/V$; the separation at lower values is believed to be a Mach number effect and is the subject of further investigation involving tests in both air and Freon.

These tests were made on semispan models rigidly mounted on the tunnel wall. The lowest identifiable frequency in the strain-gage output is that of fundamental bending and the buffeting should therefore be comparable to that in flight. A comparison with flight has been made by using the data of figure 8 and that of other angles of attack; the range of reduced frequencies covered in the comparison is indicated by the mean line. The wind-tunnel data were used to estimate the buffet loads on the X-3 airplane. The results are shown in figure 9. The circles represent values of root-mean-square bending moment measured during a 1 g stall at constantly decreasing airspeed plotted against angle of attack. The change in Mach number during the run is indicated by the arrows. The wind-tunnel results have been scaled on a dynamic basis. The comparison again is considered to be promising, although there are several factors which may be of importance but which are not assessed by these tests. For example, there were differences between flight and wind-tunnel Mach numbers at a given reduced frequency, and the aspect ratio of the airplane was smaller than that of the models. Both of these factors are believed to require further study.

CONCLUDING REMARKS

The present study has summarized the available data on the use of model tests as an indicator of the magnitude of buffet loads. The strain-gage technique, applied to both an unswept and a swept configuration, appears promising, and its use appears to be indicated in those wind tunnels with suitable flow characteristics.

Statistical concepts provide a valuable guide in the analysis of flight-test data, and scaling of the wing loads on a simple dynamic basis, which employs the methods of generalized harmonic analysis, appears to be feasible.

Langley Aeronautical Laboratory,
National Advisory Committee for Aeronautics,
Langley Field, Va., April 26, 1955.

REFERENCES

1. Press, Harry, and Houbolt, John C.: Some Applications of Generalized Harmonic Analysis to Gust Loads on Airplanes. Preprint No. 449, S.M.F. Fund Preprint, Inst. Aero. Sci., Jan. 25-29, 1954.

2. Liepmann, H. W.: On the Application of Statistical Concepts to the Buffeting Problem. Jour. Aero. Sci., vol. 19, no. 12, Dec. 1952, pp. 793-800, 822.

3. Miles, John W.: An Approach to the Buffeting of Aircraft Structures by Jets. Rep. No. SM-14795, Douglas Aircraft Co., Inc., June 1953.

4. Huston, Wilber B., and Skopinski, T. H.: Measurement and Analysis of Wing and Tail Buffeting Loads on a Fighter-Type Airplane. NACA TN 3080, 1954.

QUANTITATIVE EVALUATION OF BUFFETING

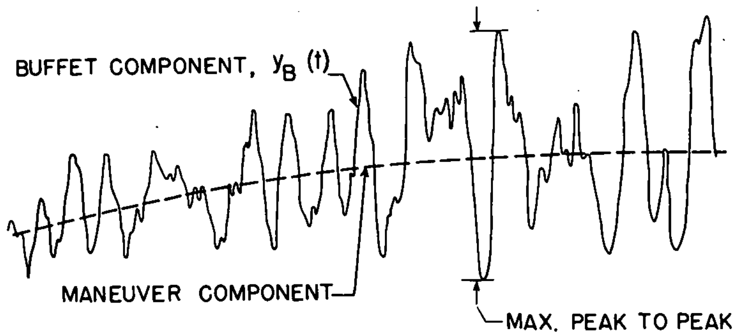

$$\sigma(t) = \left[\frac{1}{2T} \int_{t-T}^{t+T} y_B^2(t)\,dt \right]^{1/2}$$

Figure 1

FREQUENCY CONTENT OF WING BUFFET LOADS

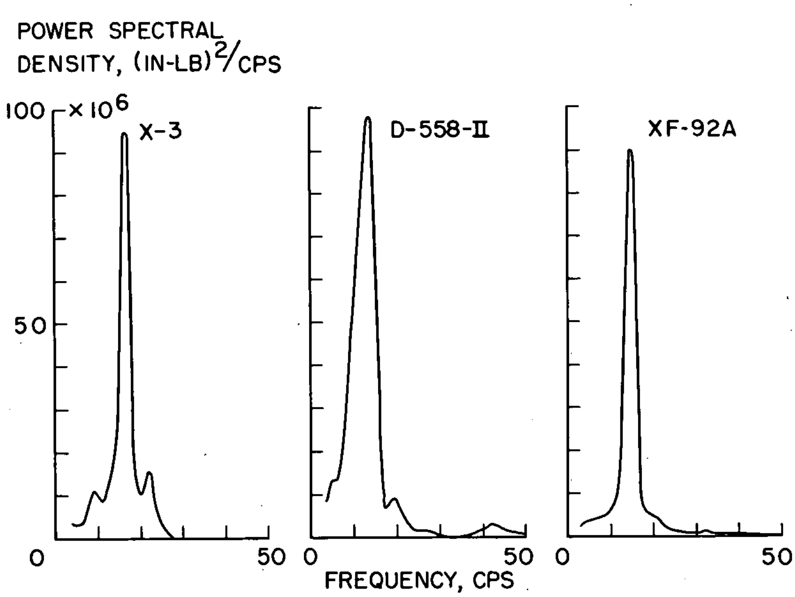

Figure 2

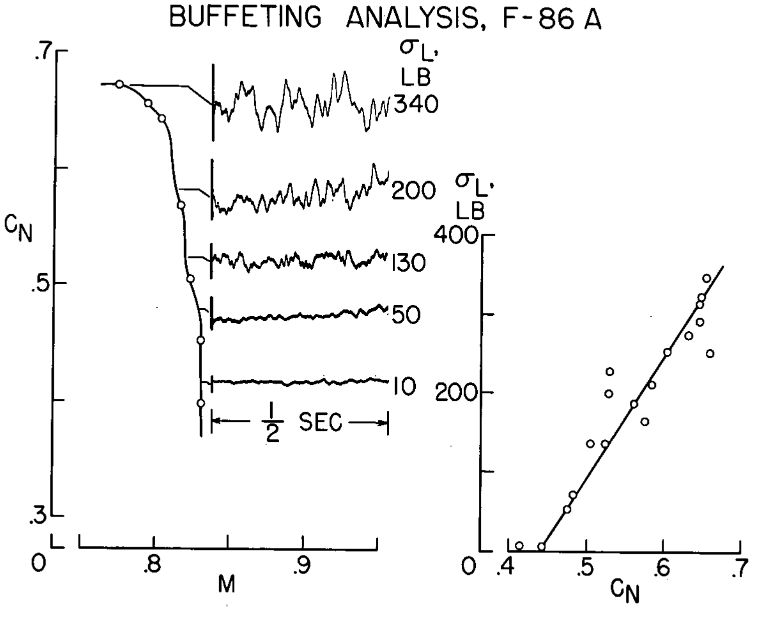

Figure 3

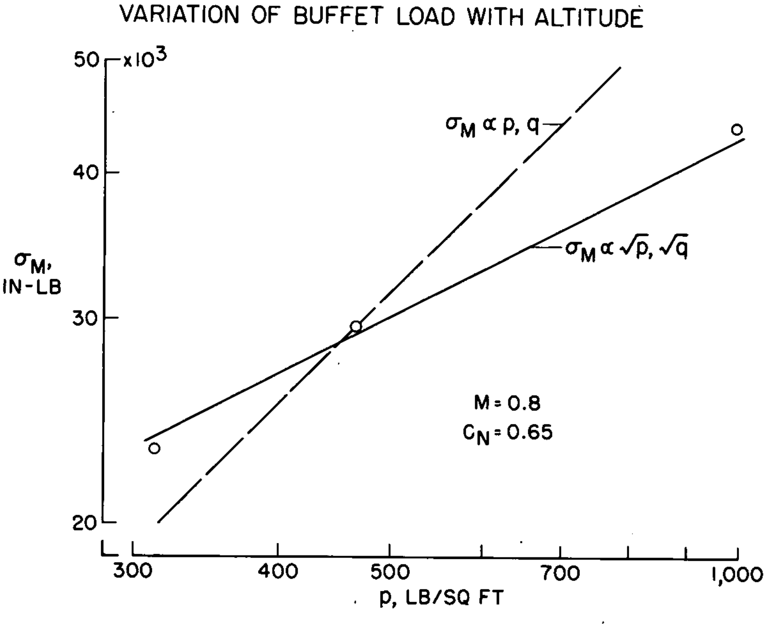

Figure 4

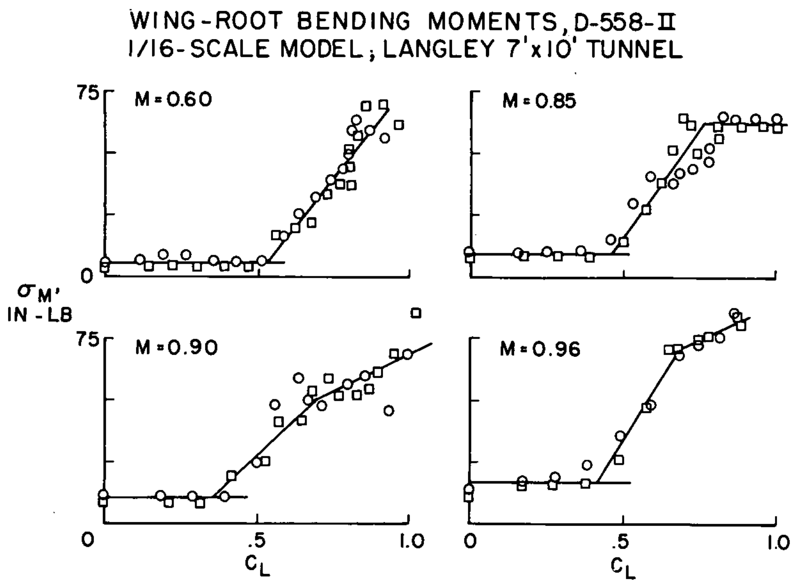

Figure 5

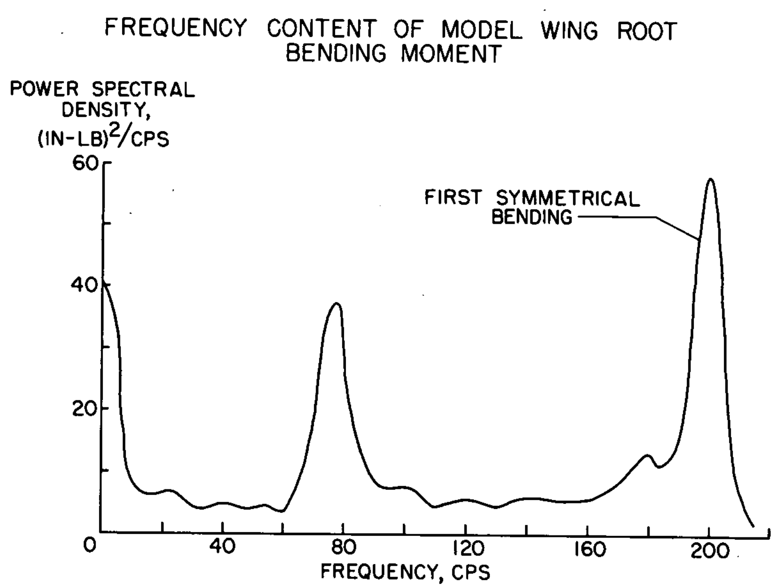

Figure 6

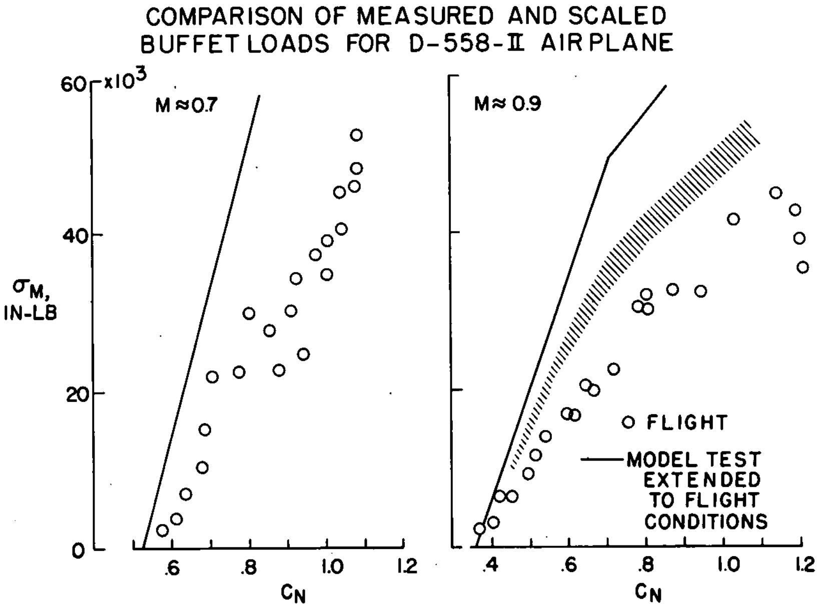

Figure 7

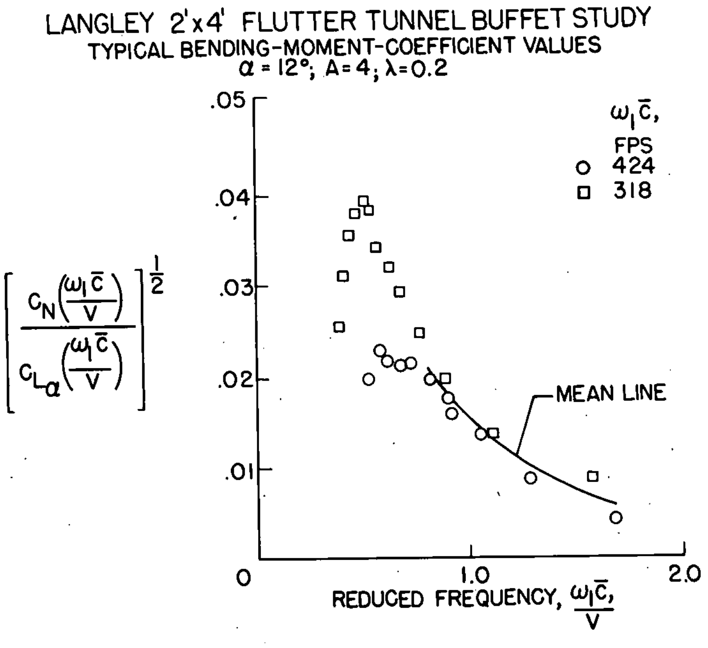

Figure 8

COMPARISON OF MEASURED AND SCALED BUFFET LOADS FOR X-3 AIRPLANE

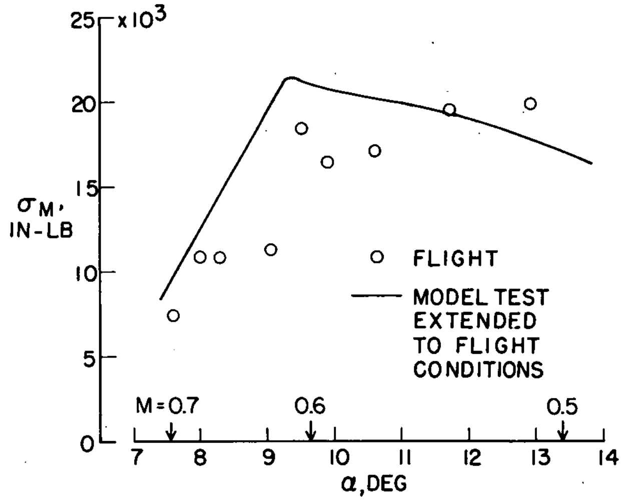

Figure 9